Atomistic potential for adsorbate/surface systems: CO on Pt

Atomistic potential for adsorbate/surface systems: CO on Pt

P. van Beurden,* H. G. J. Verhoeven, and G. J. Kramer†
Schuit Institute of Catalysis, Eindhoven University of Technology, P.O. Box 513, 5600 MB Eindhoven, The Netherlands

B. J. Thijsse
Laboratory of Materials Science, Delft University of Technology, Rotterdamseweg 137, 2628 AL Delft, The Netherlands
(Received 22 July 2002; revised manuscript received 13 September 2002; published 16 December 2002)

An atomistic interaction potential for adsorbate/surface systems is presented, based on the modified embedded-atom method (MEAM) and applied to CO on Pt. All parameters are determined using both density-functional theory (DFT) calculations, as well as the necessary experimental data. Whereas current DFT implementations suffer from problems in predicting the correct adsorption site of CO on Pt{111}, the current MEAM potential quantitatively describes the adsorption energies on the Pt {100} and {111} surfaces. With this potential, one is able to model, amongst others, diffusional properties and the CO induced lifting of the Pt{100}-hex surface reconstruction.

DOI: 10.1103/PhysRevB.66.235409 PACS number(s): 68.43.Bc, 68.43.Fg, 82.20.Wt

I. INTRODUCTION

This paper is concerned with the derivation of potential-energy parameters for a carbon monoxide adsorbate layer on platinum, within the framework of the modified embedded-atom method (MEAM) developed by Baskes.[1] The MEAM has proven to be able to cover a wide range of bulk and surface systems.[2–7] While the original parametrization by Baskes for metals and binary alloys was based on empirical data, we have shown that improved parameters can be derived by fitting to (additional) theoretical data, in particular from density-functional (DFT) calculations.[6] We here extend that methodology to parametrize a adsorbate/metal system (CO/Pt), for which parametrization can only be done by using a combination of empirical (experimental) and theoretical (DFT) results. The motivation of this work is to be able to model the complex phenomena of adsorbate-induced reconstruction of metal surfaces that have attracted much attention, especially since the advent of scanning tunneling microscopy.

The MEAM parametrization method that we present here should be applicable to a multitude of adsorbate/metal species, but we have chosen CO/Pt as a first example since it is one of the most intensively studied systems in surface science; the oxidation of CO on Pt has a similar archetypal role in catalysis (excellent overviews of both aspects are given by Ertl, and Imbihl and Ertl in Refs. 8,9). The subject is at once simple in terms of its constituent elements—simple molecules and well-characterized surface(s)—as well as rich in resulting phenomenology, such as complex adsorbate-induced restructuring and spatiotemporal oscillation of reaction rates. The experimental studies of the CO/Pt system have been supplemented by theoretical work, which has lead to a proper fundamental understanding of these processes.[8–11] An example of recent progress in this area is the elucidation of the mechanism behind the CO-induced lifting of the Pt{110}-(1×2) missing row reconstruction by Thostrup *et al.*[11] using DFT and Monte Carlo (MC) simulations. The counterpart of this reconstruction on the {100} surface, however, is a more tedious exercise due to the fact that the symmetry of the surface lattice changes from square to hexagonal, which makes a lattice-gas method (as the Monte Carlo study mentioned above) impossible—or at least inaccurate at the atomic level. It can therefore only be modeled realistically at the atomic level when accurate force fields are available.

As said, the (square) Pt{100} surface exhibits—when exposed to vacuum—a surface reconstruction in which the surface atoms adopt a quasihexagonal closest packing and as a consequence, the surface plane contains $\sim$20% more atoms than the unreconstructed square phase. Upon adsorption of CO (and several other adsorbates), this ''hex'' reconstruction is lifted by forcing the excess Pt atoms out of the plane. This is also referred to as ''restructuring'' or ''deconstruction.'' The expelled Pt atoms can, by surface diffusion, coalesce into islands and form steps.[12] Furthermore, the deconstruction proceeds anisotropically,[13,14] and its rate depends in a highly nonlinear way on the local CO coverage.[15] The underlying mechanism obviously involves a variety of atomic rearrangement processes, impossible to cover all with a lattice-gas model, such as the MC approach used for the Pt{110} case.[11] In studying these and similar mechanisms, classical molecular dynamics (MD) simulations using effective force-field potentials are essential.[16–19] Here, the derivation of such a force-field potential is described, with applications to surface diffusion and reconstruction.

The organization of this paper is as follows. In Sec. II, the experimental and theoretical data of the CO/Pt system to which the potentials are fit are introduced and—where relevant—their uncertainty is discussed. This section also contains a technical discussion of the main differences between the monoatomic and heteroatomic MEAM. Further, the physical interpretation of some of the parameters is addressed, as well as the method to determine their values. Section III describes the computational techniques regarding the DFT and MEAM simulations. In Sec. IV, the CO/Pt potential is tested and its application to the Pt{100} surface restructuring is discussed.

II. DERIVATION OF MEAM PARAMETERS

In this section, we introduce the most characteristic features of the CO/Pt systems and extend the MEAM parametrization scheme for monoatomic fcc metals to the heteroatomic system adsorbate/surface system. Although it is applied to CO/Pt here, the method has the potential to be used for other adsorbate/surface systems as well.

A. The CO/Pt system

According to several experimental studies, CO generally prefers binding at low-coordination sites, such as on-top of a Pt atom or bridging two Pt atoms. The data available for adsorption energies at these sites however, is not conclusive. For instance, Yeo *et al.*[20] find, using calorimetric measurements, an adsorption energy of -1.94 eV for CO on Pt{111}, whereas Ertl *et al.*[21] from isosteric measurements find -1.40 eV. The calorimetric measurements were performed for a series of Pt surfaces, including the Pt{100}-hex surface,[22] which makes, at least, comparison of the relative differences of the adsorption energies physically reliable and hence suitable to use in the fitting procedure. Unfortunately it is experimentally not possible to determine the difference in adsorption energy between the atop and bridge sites in a straightforward manner. Schweizer *et al.*[23] determined from their infrared measurements, using an empirical model, that binding on Pt{111} at the atop site is preferred by ~ 60 meV relative to the bridge. On Pt{100}, Martin and co-workers[24] find, using infrared spectroscopy, at a CO coverage of 0.5 monolayers (ML), a mixture of domains of all bridge or all atop species but the relative proportions of each vary as a function of temperature with the bridge domains being favored at the lowest measured temperature, 90 K. This indicates that the difference in binding energy between the two sites is rather small and in the present work, we arrived at a CO/Pt potential for which the bridge site is preferred over the atop site by no more than 0.04 eV, in the limit of zero coverage. More intriguing still, is the experimental fact that CO binds stronger to the eight-coordinated {100} surface than to both the more closed nine-coordinated {111} surface and the more open (and thus generally more reactive) seven-coordinated {110} surface.[25]

Theoretical treatment of the CO on Pt system is far from trivial, as evidenced by the conclusion of Feibelman *et al.*,[26] that current DFT implementations underestimate CO's preference for low-coordination binding sites on Pt{111}. In their extensive review, Feibelman and co-workers show that CO is, without exception, found to favor hollow over atop site adsorption, contradicting experimental studies. Although not as pronounced as Pt{111}, we have found that the Pt{100} surface suffers from similar problems in the sense that binding at the atop site is underestimated, Table I. Some limited empirical descriptions of the CO/Pt interaction exist,[23,27] but to our knowledge, no realistic CO/Pt potential has been constructed yet.

As will be discussed in Sec. II C, DFT calculations show that the lateral CO-CO interaction is rather insensitive to the site and surface the CO molecules are adsorbed on. Furthermore, in agreement with experiment,[28] the interaction has been found to be pairwise in nature: the (repulsive) energy increases proportionally with the number of CO-CO interactions. This phenomenon is a feature of the ''Pauli repulsion'' picture, in which two CO molecules are so close that the wave functions associated with their closed shells overlap.

TABLE I. DFT values for the adsorption energy of CO on Pt. The Pt surface is kept fixed to mimic electronic effects only. As explained in Ref. 26, binding to the lower-coordinated sites is generally underestimated by current DFT implementations, especially for Pt{111}.

Site	DFT (PW91)	Experiment
{100} top	-1.77	$\geqslant -2.28$
{100} bridge	-2.05	-2.28
{100} hollow	-1.50	
{111} top	-1.51	-1.94
{111} bridge	-1.62	-1.88 [a]
{111}-fcc hollow	-1.70	

[a]Adsorption energy is obtained from empirical difference between {111} bridge and atop sites according to Ref. 23.

The potential presented in this work, defined within the framework of the modified embedded-atom method, which we will elaborate on more in depth in the following section, is in principle able to describe the most relevant properties. In the present work, we choose a parametrization based on {111} and {100} reference data. Since CO binds invariably to the Pt surface atoms via the C atom, we simplified the system by considering CO as an effective atom, leaving only two different ''atoms'' participating in the system. The CO to Pt distance is then defined as the distance between the CO center of mass and Pt. In the current implementation of the MEAM, we incorporate only nearest-neighbor (NN) interactions. This implies that CO on-top of a Pt atom, cannot distinguish whether this Pt atom is part of, e.g., a {100} surface, or a {110} surface. Therefore, the difference in adsorption energy is entirely governed by the Pt atom to which CO is adsorbed. Within the concept of bond order and bond-order correction, which is at the heart of the MEAM,[6] reactivity of the Pt atom is in first instance determined by its number of NN's. Therefore, within the current NN model, the {110} surface, with only seven Pt—Pt bonds, will always be more reactive towards any adsorbate molecule than the {100} surface, with 8 Pt—Pt bonds. Consequently, no CO/Pt parametrization will be able to describe the correct order of reactivity of the different surfaces when interactions are limited to NN's only. Thus, when parametrization is based on properties of the CO/Pt{111} and CO/Pt{100} surfaces, bonding to the {110} surface will always be overestimated. Alternatively, one could choose to use CO/Pt{110} properties to fit the MEAM parameters to, but this will result in an underestimation of CO binding on Pt{111} and Pt{100}.

B. The MEAM

In the present introduction of the MEAM,[1] we will just briefly discuss the general concept for monoatomic systems and more extensively the current heteroatomic case.

In the formalism of the MEAM, the total potential energy of a system of atoms is generally written as

$$E=\sum_i E_i=\sum_i \left[\frac{1}{2}\sum_{j(\neq i)} \phi_{ij}(r_{ij})+F_i(n_i)\right], \tag{1}$$

where E_i is the energy of atom i, which depends on its environment by means of a pair potential ϕ_{ij} between atoms i and j, and bond-order energy F_i. The multibody interaction F_i, originally termed embedding energy, depends on the effective coordination number n_i of atom i. This number is constituted by the electronic density and the spatial distribution of the neighboring atoms. In the following equations we will denote, in order to generalize for any adsorbate/metal system, CO by A and Pt by M. The labels i and j denote both ''atom'' types. The bond-order energy F_A for CO is, apart from a scaling constant, equivalent to F_M for metallic elements,

$$F_A(n_A)=E_0^A\frac{n_A}{N_0^A}\ln\left(\frac{n_A}{N_0^A}\right), \tag{2}$$

where E_0^A and N_0^A are fit parameters. This functional form for F has been shown previously,[6] to correctly describe the bond-order conservation principle[29] (BOCP) in metallic systems. In general, one uses a reference system, such as the ideal fcc crystal, to assign physical meaning to the basic fit parameters. In that case, E_0 and N_0 denote, respectively, the sublimation energy and the number of nearest neighbors in the reference system (e.g., $N_0=12$ for a fcc or hcp metal). For CO, such an obvious reference system cannot be assigned, and therefore the derivation and physical interpretation of the individual parameters of F is not straightforward. In the present work, we have found that a proper description of the CO/Pt system is obtained when F_A, as well as ϕ_{AA} and ϕ_{AB}, is parametrized using a system where CO is adsorbed on Pt, rather than using an isolated CO reference system. The drawback, however, is that the physical meaning of the CO parameters in Eq. (2) is not very clear.

Due to the lack of multibody character in the CO-CO interaction energy mentioned in Sec. II A, the (multibody) bond-order energy F_A of CO, unlike F_M of Pt, is chosen to include only effects of the Pt surface atoms, i.e., n_A consists solely of neighboring Pt atom contributions. Consequently, the CO-CO interaction is entirely described by the ϕ_{AA} pair-potential. This interaction energy has been found experimentally and theoretically to be repulsive and to decay exponentially with increasing CO-CO distance, so that ϕ_{AA} (denoted as ϕ_A) can be defined as

$$\phi_A(r)=\phi_0^A e^{-\gamma_A r}, \tag{3}$$

where ϕ_0^A is a preexponential factor, γ_A describes the exponential decay of the lateral repulsion, and r denotes the CO–CO distance.

In monoatomic metallic systems, one often uses the universal equation of state as derived by Rose and co-workers[30] to derive ϕ.[1] For heteroatomic systems, the choice for ϕ_{ij} is less obvious. In a first attempt, Baskes proposed to construct a pair potential for bimetallic alloys by taking some average form of two monoatomic pair potentials.[1] For adsorbate/surface systems, this approach is not likely to be very successful, since especially the physical properties of the adsorbate drastically change compared to the desorbed gaslike state. We have therefore chosen to fit the parameters of some functional form directly to the available DFT and experimental reference data of the CO/Pt system. This *functional form* (and not the *physical interpretation*) we use, is simply a Rose-like function (alternatively, one could choose a Lennard-Jones or Morse potential). Then

$$\phi_{AM}(r)=-E_0^{AM}[1+a_{AM}(r)]e^{-a_{AM}(r)}, \tag{4a}$$

where

$$a_{AM}(r)=\alpha_{AM}\left(\frac{r}{r_0^{AM}}-1\right). \tag{4b}$$

Here, E_0^{AM} is related to energy of adsorption, α_{AM} relates to the rigidity of adsorbed CO and therefore to vibrational properties of the CO—Pt bond, and r_0^{AM} relates to the CO—Pt distance.

In comparison with previous forms, the effective coordination number for Pt n_M is extended with a smoothed step function S, in order to prevent unphysical behavior due to too small or even imaginary values for n,

$$n_M=n_M^{(0)}\sqrt{1+S(\Gamma_M)\Gamma_M};\quad S(\Gamma)=\begin{cases}1 & \text{for } \Gamma>0\\ 0 & \text{for } \Gamma<0.\end{cases} \tag{5}$$

Here, $n_M^{(0)}$ is the zeroth-order contribution to n and Γ contains effects of directional bonding. Γ is essentially the modification to the embedded-atom method (EAM) and is constituted by angular contributions $n^{(k)}$, with $k=1-3$,

$$\Gamma_M=\sum_{k=1}^{3} w_M^{(k)}\left(\frac{n_M^{(k)}}{n_M^{(0)}}\right)^2, \tag{6}$$

where $w_M^{(k)}$ are weighting factors. Although described in detail in Refs. 1,6, we give for sake of completeness as an example the first-order angular contribution to n,

$$(n_M^{(1)})^2=\sum_{j,l(\neq i)} \rho_j^{(1)}(r_j)\rho_l^{(1)}(r_l)\cos(\theta_{jil}), \tag{7}$$

where $\rho_j^{(1)}(r)$, defined below, is the first-order correction to the electronic density of atom j at distance r_j from the atom under consideration. θ_{jil} is the angle between atoms i,j, and l.

As explained above, the effective coordination number n_A of CO contains only contributions of Pt atoms. Further, since the number, and not the angular configuration, of CO's Pt

neighbors has proved to be the dominant factor, we neglect angular dependencies by setting $\Gamma_A=0$, thereby describing n_A effectively in the EAM limit,

$$n_A=n_A^{(0)}=\sum_{j\in M}\rho_j^{(0)}(r_j), \tag{8}$$

where $\rho_j^{(0)}(r)$ is the zeroth-order electronic density of Pt atom j at distance r_j from the CO molecule under consideration.

For the Pt atoms, a description that does include $k>0$ terms is essential, because CO lifts the quasihexagonal reconstruction on the Pt{100} surface, and it has been established previously,[6] that the $k=2$ contribution to the effective coordination number n plays a determining role in the stabilization of the hexagonal overlayer on the square {100} substrate. In this respect, it seems logical to disrupt this stabilizing effect by introducing (at least) a $k=2$ contribution from these specific adsorbate molecules to the metal atoms. Contributions from $k=1,3$ may also be included, but would require a larger data set for fitting, including for example data on binding of CO to steps or kinks. In general, it is not to be expected that these additional angular contributions $k=1,3$ to n will drastically improve the robustness of the description. Moreover, one should see to it that properties *not* included in the reference fit data—such as diffusion—are correctly predicted. The electronic-density contribution of a CO molecule to the effective coordination number of Pt is therefore written as

$$\rho_A^{(k)}(r)=f_A\exp\left[-\beta_A^{(k)}\left(\frac{r}{r_0^A}-1\right)\right],\quad k=0,2, \tag{9}$$

where electronic decay parameters $\beta_A^{(0)}$ and $\beta_A^{(2)}$, and distance parameter r_0^A (usually the equilibrium A-A distance in some reference structure) are to be determined. In monoatomic systems the value of electron-density amplitude f is irrelevant, since it cancels out of the coordination number ratio in F of Eq. (2), where N_0 is equivalent to the equilibrium background density defined in Ref. 1 which is proportional to f. However, when different types of atoms interact, the value of f becomes an issue.

C. Determination of CO/Pt parameters

Due to the lack of cubic symmetry in the CO/Pt system, an obvious separation of parameters is not possible.[1] Therefore, most CO and CO-Pt parameters have to be fitted *simultaneously* to the available reference data. Such a procedure implies that most of the CO-specific parameters depend implicitly on the value of the previously determined Pt parameters. For this Pt potential, the parameter sets of Ref. 1 or Ref. 6 could be used. Here, we use a slightly altered parameter set for Pt, based on the scheme described in Ref. 6, but fit to a slightly different set of reference data: instead of using the DFT value for the vacancy formation energy E_v^f, an average of experimental values,[31] 1.45 eV, has been used. This potential parametrization represents the physical properties of the Pt{100} better than the previous potential, which tends to overestimate binding energies within the hexagonally reconstructed surface layer.

TABLE II. Experimental data and the resulting MEAM fit values. Experimental data taken from Refs. 20,22, where calorimetric heats of adsorption were measured at CO coverages of 0.01 to 0.04 ML. Also listed, the MEAM values after allowing the Pt surface atoms to relax, at CO coverages around 0.01 ML.

Site	Experiment	MEAM fit	MEAM after relaxation
{100} top	$\geqslant -2.28$	-2.20	-2.24
{100} bridge	-2.28	-2.24	-2.28
{100} hex	-2.00		$\langle -2.05\rangle$ [a]
{111} top	-1.94	-2.09	-2.12
{111} bridge	-1.88 [b]	-1.90	-2.03
{110} top	-2.00		-2.35 [c]
{110} bridge	$\geqslant -2.00$		-2.44 [c]

[a]Averaged value for different bridge and atop sites of hexagonally reconstructed surface. This value is not included in the fit.

[b]Adsorption energy is obtained from empirical difference between {111} bridge and atop sites according to Ref. 23.

[c]Bonding of CO to Pt{110} is overestimated due to the restriction of the interaction to nearest neighbors. Details are explained in the text.

The CO/Pt reference data include adsorption energies and lateral interactions on the {100} and {111} surfaces, see Table II and Figs. 1 and 2. Although not explicitly mentioned, the adsorption energies on the threefold and fourfold hollow sites are considerably higher than on the lower-coordination sites (in the order of 0.5 to 1 eV). The resulting MEAM parameters for CO and CO/Pt are shown, together with the Pt

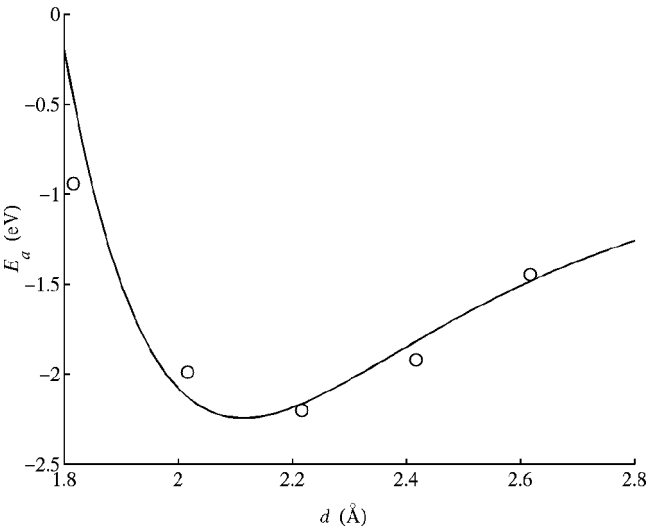

FIG. 1. Adsorption energy E_a for a CO molecule on a Pt{100}-bridge site as a function of CO to surface distance d (measured from the CO center of mass to the surface plane). The open circles represent the DFT calculations, shifted down by 0.23 eV to match the experimental value of Ref. 22. The solid line depicts the MEAM fit, used to determine the CO-Pt and most of the CO parameters listed in Table III.

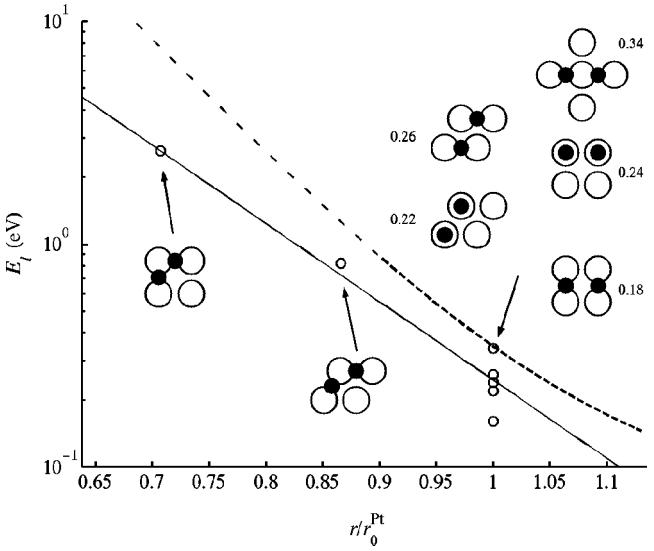

FIG. 2. Lateral CO-CO interaction E_l as a function of intermolecular separation r. r_0^{Pt} denotes the Pt NN distance. The data points represent the DFT calculations and the solid line depicts ϕ_{CO} of Eq. (3) fitted to the DFT results. The repulsion energy is proportional to the number of CO-CO bonds within a few meV. The dashed line denotes the empirical repulsion, Ref. 28, of which the dense part indicates the empirically reliable range ($r \gtrsim 0.9 r_0^{Pt}$). Several configurations are indicated, e.g., around $r = 0.71 r_0^{Pt}$, the interaction of CO molecules located at nearest bridge positions on the {100} surface, and around $0.87 r_0^{Pt}$ the CO-CO interaction at next-nearest bridge positions on {111}. At $r = r_0^{Pt}$, five configurations and corresponding energies are indicated.

parameters, in Table III and are further discussed below. Since the type of (surface) systems to which the parameters are fitted, are rather similar, some degree of arbitrariness in the fitting scheme remains unavoidable.

1. CO and CO-Pt parameters

Here, the derivation of all CO parameters except ϕ_0 and γ, and all CO-Pt parameters is described. In short, all parameters are, through the analytical MEAM expressions for the atomic energy [Eq. (1)], simultaneously fitted to the reference data of the adsorption and relaxation energies of CO on Pt{100} and Pt{111}. This procedure is similar to the case of homogeneous metallic systems, where surface energies and surface layer relaxations have been used.[6]

Some physical meaning to the CO MEAM parameters can be imposed by assigning to r_0^{CO}, e.g., the equilibrium value of the lateral CO-CO distance in the $(CO)_2$ gas-phase dimer. Since this value is larger than the value for r_0^{Pt}, the electronic density of CO, Eq. (9), is larger than the electronic density of Pt at a given distance r. A value for f_{CO} smaller than 1 may, to some extent, compensate for this effect. Although several physical plausible values for f have been proposed,[32] in this work a value of 0.5 for f_{CO} is found to properly describe the current system.

It has been shown previously, that the intramolecular C-O and the intermolecular Pt-C stretching vibrations are correctly described within current DFT implementations,[33–36] despite the fact that calculation of adsorption energies is cumbersome. This implies that the change in adsorption energy as a function of CO to Pt distance is correctly reproduced by DFT. As a result, for determining the CO and CO-Pt parameters, DFT calculations are best used after correction for the off-sets of the adsorption energies using experimental data. The interaction energy as a function of the CO distance to the Pt{100} bridge site is shown in Fig. 1. The Pt atoms have been kept fixed, in order to mimic electronic effects only.

Table II displays the empirical reference data, as well as the resulting MEAM fit to it. The adsorption energies for CO on Pt{110}, as reproduced by the current MEAM potential, are typically 0.4 eV too low compared to experiment. The reason for this artifact—in the current model inevitable—lies in the restriction to NN interactions, as explained above in Sec. II A. Despite the artifact, the general trends of the current CO/Pt potential are in better agreement with experiment than current DFT implementations and to our knowledge, no CO/Pt potentials exists which performs better.

2. CO-CO parameters

As mentioned in Sec. II A, the CO-CO interaction is pairwise and more or less independent of adsorption site and surface. Since the CO-CO interaction energy is described by just the pair potential of Eq. (3), the parameters ϕ_0^{CO} and γ_{CO} entirely define the interaction. Using DFT, the lateral interaction at different coverages and adsorption sites can easily be calculated for both the {100} and {111} surfaces. Again, to separate the electronic effects from the atomic relaxation effects, the Pt surface is kept fixed and only the C and O atoms are allowed to relax their interatomic distances perpendicular to the surface plane. The results are summarized in Fig. 2 and agree reasonably well with the empirical relation for CO on Pt{111} derived by Persson *et al.*[28] Part of the discrepancy between the DFT calculations and the empirical data might be assigned to inhibited relaxations of the Pt surface.[27] This

TABLE III. MEAM parameters for CO and Pt. Parameters E_0 and ϕ_0 are in eV/atom, r_0 in angstrom, and γ in $Å^{-1}$. The physical interpretation of the Pt parameters is discussed in Refs. 1,6. The physical interpretation of the CO and CO/Pt parameters is discussed in the text.

	E_0	r_0	α	A	N_0	ϕ_0	γ	f	$\beta^{(0)}$	$\beta^{(1)}$	$\beta^{(2)}$	$\beta^{(3)}$	$w^{(0)}$	$w^{(1)}$	$w^{(2)}$	$w^{(3)}$
Pt	5.47	2.82	6.23	0.99	12			1	4.32	4.64	0.50	2.33	1	0.14	−1.38	6.00
CO	3.21	4.01		1	3.22	799.6	2.87	0.5	4.05		5.13		1	0.0	0.0	0.0
CO-Pt	1.77	2.40	10.75													

effect arises because an adsorbed CO molecule induces localized relaxations of the substrate lattice around the adsorption site and when another CO molecule is close enough, the perturbation caused by one CO molecule influences the other, and the total adsorption energy is not exactly the sum of the adsorption energies of the isolated adsorbates, i.e., an effective interaction energy appears. This indirect repulsion is not present in the DFT calculations, since the Pt substrate is kept fixed, see Sec. III. In MD simulations, the indirect repulsion will of course naturally emerge as a function of CO coverage (not shown here).

III. COMPUTATIONAL METHODS

The DFT calculations were performed using the VASP package,[37,38] which uses periodic cells, a plane-wave basis set, and ultrasoft Vanderbilt pseudopotentials with scalar relativistic corrections. For the GGA the PW91 functional is used. point sampling and energy cutoff. In all DFT calculations the energy cutoff was 350 eV and the ***k***-point summations were done on 15-point to 45-point meshes in the irreducible part of the Brillouin zone. For all surface calculations, five-layered periodic slabs were used. In the {100} slab, each plane contains four Pt atoms; in the {111} slab, three Pt atoms. All Pt atoms were kept fixed, as required by the fit procedure described above and to mimic electronic effects only. The CO molecules were allowed to fully relax their internal CO bond length, but kept perpendicular to the surface plane. In calculating the lateral CO-CO repulsion, the C-Pt distance was also optimized. The low coverage limit is approximated by one CO molecule per unit cell, resulting in coverages of 0.25 and 0.33 ML for {100} and {111}, respectively. From the lateral CO-CO interactions and from the $(CO)_2$ gas-phase dimer calculations, it follows that the interaction vanishes around 4 Å, approximately equal to the next-nearest-neighbor distance of Pt. Therefore, it may be assumed that these coverages represent the zero coverage limit reasonably well, also taking into account the fact that the Pt substrate is not allowed to relax.

The MEAM calculations were performed using the CAMELION code as developed by Thijsse and co-workers.[39] CAMELION solves Newton's equations of motion and applies the velocity-verlet algorithm using automatic time-step adaptation for time evolution. The interactions between atoms are in the present work restricted by NN interactions only, using a radial cutoff. The same cutoff distance is assumed for both CO and Pt. The effect of varying the cutoff distance is discussed below in Sec. IV A. The quasihexagonal surface reconstruction of Pt{100} is approximated by periodic (5×1) unit cells on top of a bulk-terminated (1×1) substrate.

IV. APPLICATIONS AND DISCUSSION

In this section, the main characteristics of the CO/Pt interaction potential are investigated by evaluating the potential-energy surfaces of CO on Pt{100} and {111}. The effect of varying the radial interaction cutoff r_c is compared with DFT calculations in order to establish a physically justified value for r_c. Further, diffusion of CO on both Pt surfaces is probed and the main concepts of the mechanism driving the CO-induced lifting of the Pt{100}-hex reconstruction are discussed. A more extensive study on the details of the dynamics and mechanism of this process will be published elsewhere.[40]

A. Potential-energy surfaces

The nature of an adsorption site, e.g., onefold (atop) or twofold (bridge), is in first instance determined by the number of Pt surface atoms interacting with the adsorbate molecule. Obviously then, this is related to the value of the interaction cutoff r_c, which must ensure that CO does not interact with, e.g., any of the four next-nearest Pt atoms when adsorbed atop on Pt{100}. The CO/Pt interaction energy at intermediate adsorption sites is therefore largely determined by the choice of the value for r_c and thus whether CO is bound to, e.g., two or three Pt atoms. The effect of varying r_c on the potential-energy surface of CO/Pt{100} is shown in Fig. 3. At lower cutoffs, an artificial local minimum in the PES starts to appear at a position between top and hollow; at higher cutoffs this local minimum vanishes. This suggests that a lower limit to r_c exists around 3.3 Å. At all relevant simulation temperatures, say $T>100$ K, this artifact should be unimportant. In order to obtain a physically justified value for r_c, the change in interaction energy when CO moves parallel to the surface from the bridge to the hollow site on Pt{100}, is compared to (shifted) DFT calculations, Fig. 4. It is concluded that, considering the accessible values of r at relevant simulation temperatures up to $\sim$1000 K, $r_c = 3.45$ Å gives the best agreement with the DFT results.

On the Pt{111} surface things are a bit more delicate still, since at the bridge position, CO is relatively close to the two next-nearest Pt atoms. In order to avoid interaction, an upper limit to r_c exists for this surface around 3.3 Å. Figure 5 displays the PES of CO on Pt{111} with this cutoff. Since, as mentioned before, DFT has problems with this specific surface, a direct comparison between the MEAM potential and DFT is not possible, as compared to the CO/Pt{100} case, where at least the ''right order'' of adsorption energies is reproduced, Table I.

Thus, depending on the surface and simulation temperature, an adequate value for r_c would be between 3.3 and 3.45 Å.

As can be seen from Figs. 3 and 5, both the bridge and atop sites are local minima, being separated by a barrier of 0.2–0.3 eV. This agrees with the conclusions of Schweizer *et al.*,[23] who estimated from their IRAS measurements a barrier of 0.3 eV between bridge and atop for CO on Pt{111}, and Ma *et al.*,[41] who find from diffraction measurements a barrier of 0.13–0.20 eV. Also, Ge *et al.*[42] calculated for CO on Pt{110} a barrier of $\sim$0.15 eV between the bridge and atop sites. Another way to compare the energy barriers to experi-

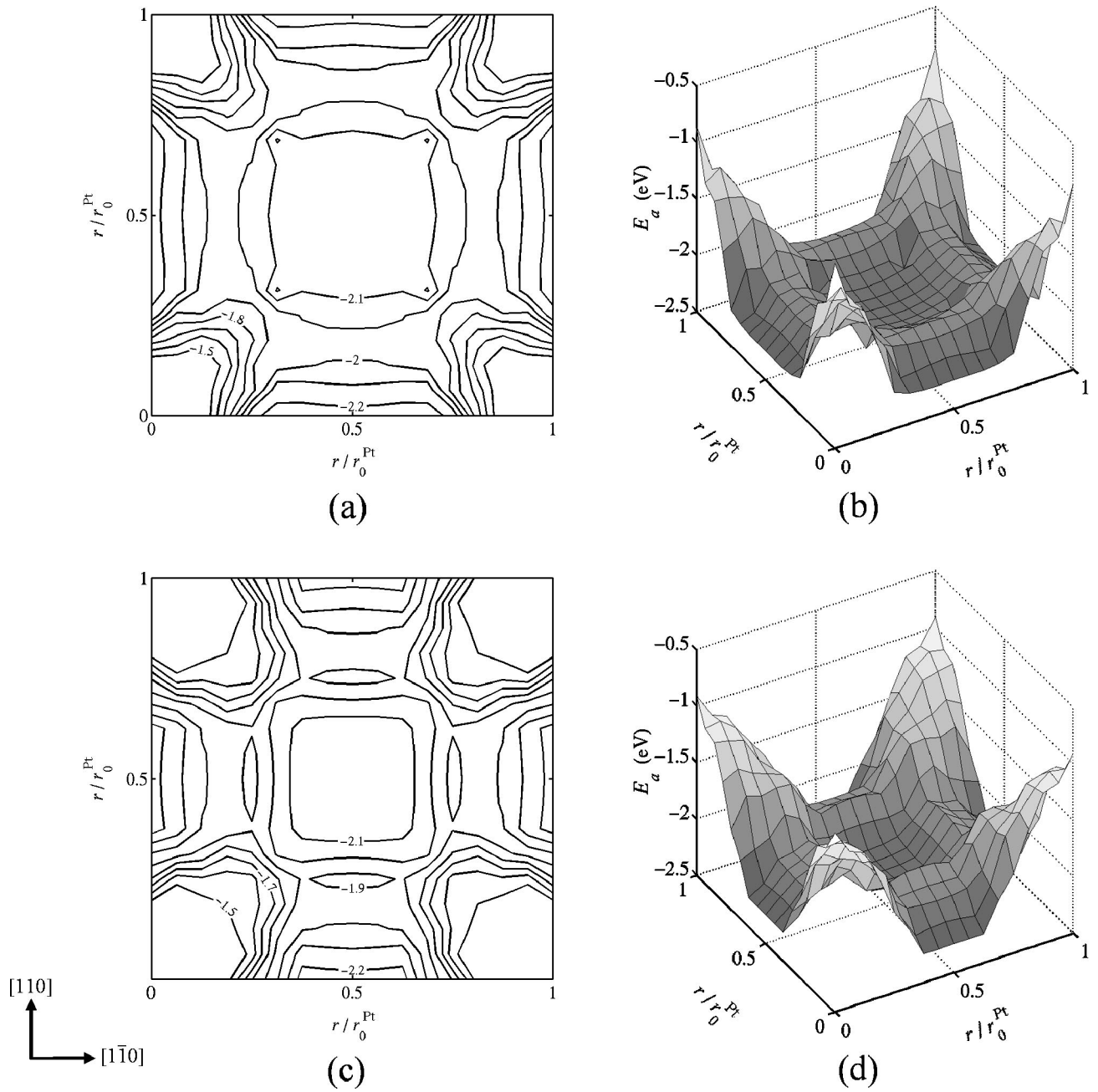

FIG. 3. 2D and 3D plots of the CO/Pt{100} potential-energy surfaces, centered around the atop site. The Pt substrate is kept fixed. r denotes the distance from the hollow site located at (0,0). In (a) and (b) the interaction cutoff r_c is 3.3 Å, in (c) and (d) it is 3.45 Å. The contour lines in (a) and (c) indicate energies ranging from -2.2 to -1.5 eV, separated by intervals of 0.1 eV. The adsorption energy at the bridge is the lowest, -2.24 eV, followed closely by the atop site, -2.20 eV.

mental data, is by obtaining the diffusion coefficient D from molecular-dynamics simulations and assuming an Arrhenius temperature dependence,

$$D = D_0 \exp(-E_d / k_B T). \tag{10}$$

Here, E_d is the energy barrier between the two local minima at the atop and bridge sites, and D_0 denotes a prefactor containing entropic contributions from the substrate. The values measured for E_d are in good agreement with the MD results, Table IV and Fig. 6. For CO on Pt{111} a wide range of values for D_0 is measured,[43] which makes quantitative comparison with our MD simulation results rather pointless. Ma *et al.* conclude from their measurements that these experimental discrepancies are caused by surface defects. Unfortunately, experimental data for diffusion of CO on Pt{100} is not available at all.

As can be seen, the simulated values of D_0 and E_d for CO/Pt{111} are larger than for CO/Pt{100}. This might be related to the fact that, compared to the atop site, the local minimum at the bridge site on {111} is higher than on {100}, which causes CO on {111} to effectively hop from atop to

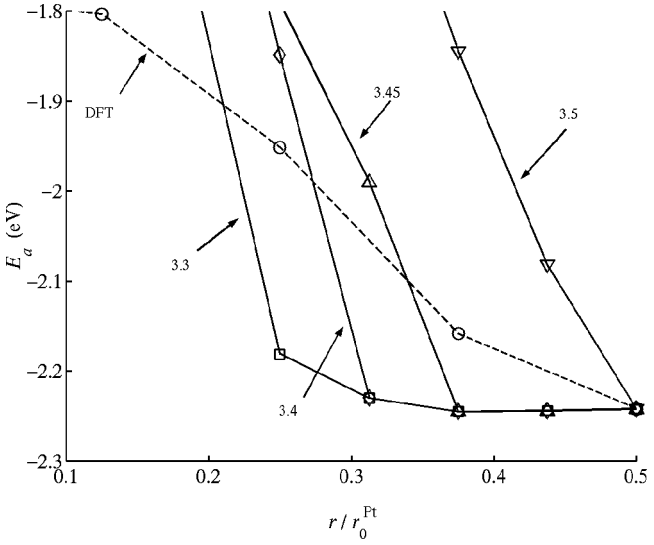

FIG. 4. Adsorption energy E_a as a function of the distance from the hollow site. At $r=0.5r_0^{Pt}$ the bridge site is located. The dashed line indicates the DFT calculations, the solid lines depict the MEAM calculations with different interaction cutoffs r_c as indicated by the arrows. A cutoff around 3.4 Å gives the best agreement with DFT calculations.

atop site, passing a higher-effective barrier and, by skipping the bridge site, resulting in a larger hop length and thus larger D_0. On the other hand, in the Arrhenius plot, the simulation values of CO/Pt{111} are more scattered than those of CO/Pt{100}, resulting in a considerably larger statistical error for D_0 and E_d of {111}, which makes direct comparison more difficult.

B. CO-induced restructuring of Pt{100} hex

The adsorbate-induced lifting of the Pt{100}-hex surface reconstruction is among the most intensively studied surface phenomena (see for instance Refs. 13–15,24,46–48 and references therein). The hex phase contains approximately 20% more Pt atoms than the bulk-terminated (1×1) phase. One of the most pronounced features of the CO-induced restructuring, as observed in STM measurements,[13,14] is the highly anisotropic growth of (1×1) domains on the otherwise (quasi) hexagonal surface. Despite the initial controversy, the nucleation of the restructuring is concluded to occur at (specifically oriented) defects at the surface.[14] Although many details of the underlying mechanism have been revealed, an atomistic model is still lacking.

Studying the mechanism behind the surface restructuring with lattice-gas methods, such as Monte Carlo (MC), is doomed to failure, due to the large variety of possible elementary steps involved in the displacement of the excess Pt surface atoms, and due to the complexity of the overall change in surface density and structure. It should be mentioned, however, that the more straightforward mechanism describing the CO-induced lifting of the Pt{110}-(1×2) reconstruction *can* be modeled using MC,[11] since the processes involved there are less complicated and more evident. Also, when incorporating the surface reconstruction in an effective way, the CO oxidation reaction can be modeled as well, using lattice-gas methods.[10,49–52] Classical molecular-dynamics simulations, using the proper effective potential, would be the obvious method to study such processes.

Using a periodic slab with a stepped Pt{100}-hex surface, MD simulations with our MEAM potential for CO/Pt indeed reveal an anisotropic mechanism for the phase transition. In

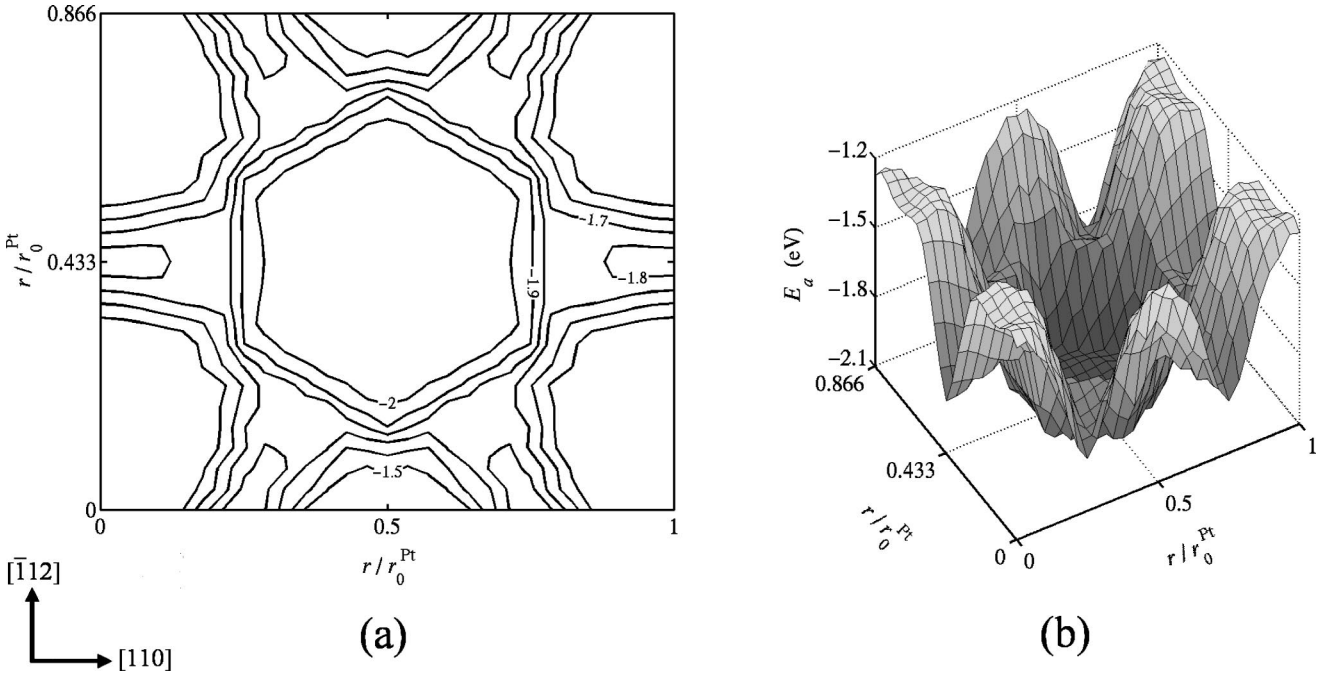

FIG. 5. 2D and 3D plots of the CO/Pt{111} potential-energy surfaces, centered around the atop site. The Pt substrate is kept fixed and the interaction cutoff r_c is 3.3 Å. The contour lines in (a) indicate energies ranging from -2.1 to -1.5 eV, separated by intervals of 0.1 eV. The adsorption energy is lowest at the atop site, -2.09 eV. The local energy minimum at the narrow bridge sites is -1.90 eV.

TABLE IV. Diffusion parameters D_0 (cm^2/s) and E_d (eV) for CO on the Pt {100} and {111} surfaces. MEAM-1 denotes the results of MD simulations with an interaction cutoff r_c of 3.3 Å and MEAM-2 denotes the results with $r_c = 3.45$ Å. The standard errors in the fit parameters are considerably larger for {111} than for {100}. Obviously, the effect of varying cutoff is small. Experimental data for the {100} surface are not available. For the {111} surface the experimental values for D_0 and for E_d vary significantly, depending on the surface coverage and the applied technique, Ref. 43.

	Expt. [a]		MEAM-1		MEAM-2	
System	D_0	E_d	D_0	E_d	D_0	E_d
CO/Pt{100}			$1.4\times10^{-4\pm0.3}$	0.26 ± 0.04	$8.7\times10^{-5\pm0.5}$	0.21 ± 0.07
CO/Pt{111}	$1\times10^{-6}, 7\times10^{-1}$	0.17,0.54	$4.0\times10^{-3\pm0.9}$	0.43 ± 0.13		

[a]See Refs. 44,45, respectively.

Fig. 7 it is clearly visible that excess Pt atoms of the hex phase are *collectively ejected* in chains from the surface to form chains adatoms, which indicates that the restructuring mechanism is nonlocal, extending over several atoms, instead of a local, isolated phenomenon, as usually assumed in MC simulations.[10] The observed process makes sense when one realizes that with a collective ejection of atoms, fewer Pt—Pt bonds are broken than in the case of ejection of a single Pt atom from the surface. In addition, no excessive mass transport is required, apart from a local rearrangement of the remaining surface atoms.

Of course, one may argue that binding of CO to the lower-coordinated Pt atoms in the ejected chains is overestimated, as exemplified by CO binding to Pt{110}, Table II. But then again, this would also hold for single, isolated adatoms. Therefore, this overestimated binding to lower-coordinated Pt atoms would, at worst, result in an *enhanced* restructuring mechanism, not in a *different* mechanism. Still, the strongest support for the observed mechanism comes from experiment: the resemblance with the STM images, in which similar anisotropic features are observed, is excellent (Figs. 6 and 7 in Ref. 14), which means that the phenomenon of the CO-induced lifting of the Pt{100}-hex reconstruction is successfully simulated.

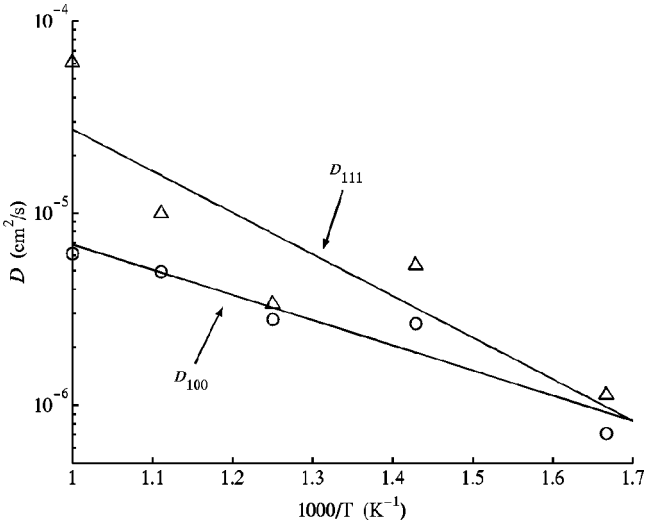

FIG. 6. Arrhenius plots of the CO diffusion on Pt{100} and {111}. In all simulations the interaction cutoff r_c is 3.3 Å (i.e., MEAM-1 in Table IV).

The details are discussed more in depth in a companion paper,[40] but it is worth noting that we find a similar nonlinear CO-coverage dependence of the restructuring rate as observed experimentally.[15] In addition, by varying the simulation temperature, an effective activation energy of 0.4 eV for the restructuring process could be estimated. This value is obviously lower than the experimental value of ~1 eV for the reverse process: the reconstruction restoring the hex phase. This is in line with the experimental observations that *de*construction (simulated here) occurs at temperatures as low as 150 K,[53] whereas *re*construction occurs at higher temperatures: around 400 K.[46]

Apart from the overall agreement with experimental data, the predictive capabilities and physical reliability of the MEAM is also illustrated by the fact that when all CO is removed after the deconstruction is completed and the square bulk-terminated phase is restored, the surface starts to reconstruct again to the hex phase, by ''absorbing'' the adatom chains directly into the surface. Although this is the exact reverse of the deconstruction mechanism, in reality the adatom chains will condense into larger and more stable islands before all CO can be removed. Then different mechanisms for reconstruction will become more important.

V. CONCLUDING REMARKS

The results discussed above support the idea that the CO/Pt MEAM potential presented in this work can be successfully applied in MD simulations to model physical properties of CO-covered Pt surfaces. Even more, the current parametrization scheme can be expected to work for similar adsorbate/surface systems as well, such as NO on Rh, considering the adequate description of CO/Pt presented here and the previous undeniable success of the MEAM in general. Further, an extension of the interatomic interactions to next-nearest neighbors may contribute to an improved description of adsorbates on all surfaces, such that the current overestimated binding of CO to Pt{110} can be resolved.

The work presented here can therefore contribute to enhanced application of effective-potential based MD simulations in theoretical research of surface science and catalysis, a field in which MC and DFT have been the predominant techniques.

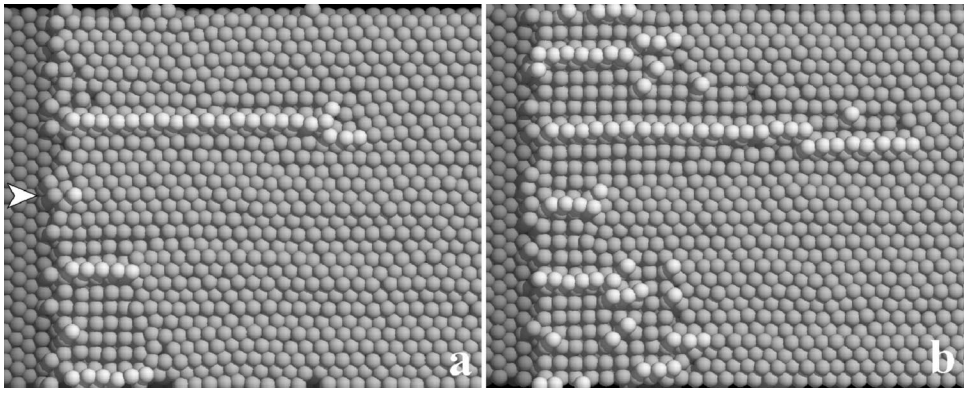

FIG. 7. MD simulation snapshots of the initial CO-induced transformation of the Pt{100}-hex reconstruction, where the excess Pt atoms are ejected in chains. For clarity CO is not shown. Darker colors represent lower levels. These simulations were performed with a surface temperature of 850 K and CO coverage of 0.5 ML, but similar behavior is found at, e.g., a temperature of 600 K and a coverage of 0.40 ML. The transformation is nucleated at the step (marked by the arrow) and proceeds anisotropically with the preferred direction perpendicular to the step. The resemblance with the STM images by Borg *et al.* is remarkable (Ref. 14).

ACKNOWLEDGMENTS

The authors would like to thank J. Hafner for providing us with the VASP package. This work was sponsored by the NWO/SPINOZA fund; G.J.K. acknowledges the financial support of Shell Global Solutions International B.V. This work was performed under the auspices of NIOK, The Netherlands Institute for Catalysis Research.

*URL: http://www.catalysis.nl/~paul
†Electronic address: Gert.J.Kramer@opc.shell.com

[1] M. I. Baskes, Phys. Rev. B **46**, 2727 (1992).
[2] M. I. Baskes, Modell. Simul. Mater. Sci. Eng. **5**, 149 (1997).
[3] M. I. Baskes, Mater. Chem. Phys. **50**, 152 (1997).
[4] K. Takahashi, C. Nara, T. Yamaghishi, and T. Onzawa, Appl. Surf. Sci. **151**, 299 (1999).
[5] T. Yamaghishi, K. Takahashi, and T. Onzawa, Surf. Sci. **445**, 18 (2000).
[6] P. van Beurden and G. J. Kramer, Phys. Rev. B **63**, 165106 (2001).
[7] M. I. Baskes and R. A. Johnson, Modell. Simul. Mater. Sci. Eng. **2**, 147 (1994).
[8] G. Ertl, Adv. Catal. **37**, 211 (1990).
[9] R. Imbihl and G. Ertl, Chem. Rev. **95**, 697 (1995).
[10] R. J. Gelten, A. P. J. Jansen, R. A. van Santen, J. J. Lukkien, J. P. L. Segers, and P. A. J. Hilbers, J. Chem. Phys. **108**, 5921 (1998).
[11] P. Thostrup, E. Christoffersen, H. T. Lorensen, K. W. Jacobsen, F. Besenbacher, and J. K. Nørskov, Phys. Rev. Lett. **87**, 126 102 (2001).
[12] W. Hösler, E. Ritter, and R. J. Behm, Ber. Bunsenges. Phys. Chem. **90**, 205 (1986).
[13] E. Ritter, R. J. Behm, G. Pötschke, and J. Wintterlin, Surf. Sci. **181**, 403 (1987).
[14] A. Borg, A.-M. Hilmen, and E. Bergene, Surf. Sci. **306**, 10 (1994).
[15] A. Hopkinson, X.-C. Guo, J. M. Bradley, and D. A. King, J. Chem. Phys. **99**, 8262 (1993).
[16] K.-D. Shiang and T. T. Tsong, Phys. Rev. B **49**, 7670 (1994).
[17] M. I. Haftel, M. Rosen, T. Franklin, and M. Hettermann, Phys. Rev. B **53**, 8007 (1996).
[18] V. S. Stepanyuk, D. I. Bazhanov, W. Hergert, and J. Kirschner, Phys. Rev. B **63**, 153 406 (2001).
[19] F. Ercolessi, M. Parrinello, and E. Tosatti, Surf. Sci. **177**, 314 (1986).
[20] Y. Y. Yeo, L. Vattuone, and D. A. King, J. Chem. Phys. **106**, 392 (1997).
[21] G. Ertl, M. Neuman, and K. M. Streit, Surf. Sci. **64**, 393 (1977).
[22] Y. Y. Yeo, L. Vattuone, and D. A. King, J. Chem. Phys. **104**, 3810 (1996).
[23] E. Schweizer, B. N. J. Persson, M. Tüshaus, D. Hoge, and A. M. Bradshaw, Surf. Sci. **213**, 49 (1989).
[24] R. Martin, P. Gardner, and A. M. Bradshaw, Surf. Sci. **342**, 69 (1995).
[25] W. A. Brown, R. Kose, and D. A. King, Chem. Rev. **98**, 797 (1998).
[26] P. J. Feibelman, B. Hammer, J. K. Nørskov, F. Wagner, M. Scheffler, R. Stumpf, R. Watwe, and J. Dumesic, J. Phys. Chem. **105**, 4018 (2001).
[27] R. Brako and D. Šokčević, Surf. Sci. **469**, 185 (2000).
[28] B. N. J. Persson, M. Tüshaus, and A. M. Bradshaw, J. Chem. Phys. **92**, 5034 (1990).
[29] E. Shustorovich, Surf. Sci. Rep. **6**, 1 (1986).
[30] J. H. Rose, J. R. Smith, F. Guinea, and J. Ferrante, Phys. Rev. B **29**, 2963 (1984).
[31] Y. Kraftmakher, Phys. Rep. **299**, 79 (1998).
[32] R. A. Johnson, Phys. Rev. B **39**, 12 554 (1989).
[33] M. T. M. Koper, R. A. van Santen, S. A. Wasileski, and M. J. Weaver, J. Chem. Phys. **113**, 4392 (2000).
[34] A. Eichler, Surf. Sci. **498**, 314 (2002).
[35] S. A. Wasileski, M. T. M. Koper, and M. J. Weaver, J. Phys. Chem. B **105**, 3518 (2001).
[36] M. T. M. Koper, T. E. Shubina, and R. A. van Santen, J. Phys. Chem. B **106**, 686 (2002).
[37] G. Kresse and J. Furthmüller, Phys. Rev. B **54**, 11 169 (1996).
[38] G. Kresse and J. Furthmüller, Comput. Mater. Sci. **6**, 15 (1996).

[39] B. J. Thijsse, computer code CAMELION (Delft University of Technology, Delft, 2001).
[40] P. van Beurden, B. S. Bunnik, G. J. Kramer, and A. Borg, Phys. Rev. Lett. (to be published).
[41] J. Ma, X. Xiao, N. J. DiNardo, and M. M. T. Loy, Phys. Rev. B **58**, 4977 (1998).
[42] Q. Ge and D. A. King, J. Chem. Phys. **111**, 9461 (1999).
[43] E. G. Seebauer and C. E. Allen, Prog. Surf. Sci. **49**, 265 (1995).
[44] J. E. Reutt-Robey, D. J. Doren, Y. J. Chabal, and S. B. Christman, J. Chem. Phys. **93**, 9113 (1990).
[45] V. J. Kwasniewski and L. D. Schmidt, Surf. Sci. **274**, 329 (1992).
[46] P. R. Norton, J. A. Davies, D. K. Creber, C. W. Sitter, and T. E. Jackman, Surf. Sci. **108**, 205 (1981).
[47] P. A. Thiel, R. J. Behm, P. R. Norton, and G. Ertl, Surf. Sci. **121**, L553 (1982).
[48] R. J. Behm, P. A. Thiel, P. R. Norton, and G. Ertl, J. Chem. Phys. **78**, 7437 (1983).
[49] V. N. Kuzovkov, O. Kortlüke, and W. von Niessen, J. Chem. Phys. **108**, 5571 (1998).
[50] V. P. Zhdanov, J. Chem. Phys. **110**, 8748 (1999).
[51] F. Cháv́ez, L. Vicente, A. Perera, and M. Moreau, J. Chem. Phys. **112**, 8672 (2000).
[52] E. I. Latkin, V. I. Elokhin, and V. V. Gorodetskii, J. Mol. Catal. A: Chem. **166**, 23 (2001).
[53] J. A. Davies, T. E. Jackman, D. P. Jackson, and P. R. Norton, Surf. Sci. **109**, 20 (1981).